

Buckling Behaviour of Randomly Corroded Stiffened Steel Plates Using Gaussian Distribution Under Uniaxial Compression

Zorareh Hadj Mohammad Esmaeil Nouri
PhD Candidate, Faculty of Marine Technology
Amir Kabir University of Technology,
Tehran 15914
Iran
nouri1360@yahoo.com
www.aut.ac.ir

Karim Moradi Dohezari
Saff-Rosemond Management & Engineering Co.
Ario Building, North Falamak, Ghods Town
Tehran
Iran
behnammoradi@yahoo.com
www.saff-rosemond.com

ABSTRACT

This paper presents the results of an investigation into the post-buckling behavior and ultimate strength of imperfect corroded steel plates used in ship and other marine-related structures. A series of elastic-plastic large deflection finite element analyses is performed on both-sides randomly corroded steel plates. The effects of general corrosion are introduced into the finite element models using a random thickness surface model considering Gaussian distribution with different standard deviation. The effects on plate compressive strength as a result of parametric variation of the corroded surface geometry are evaluated. A proposal on the effective thickness is concluded in order to estimate the ultimate strength and explore the post-buckling behavior of randomly corroded steel plates under uniaxial compression.

Key words: Buckling, Random Corrosion, Ultimate Strength, Stiffened Plate, FE Modeling.

Notations:

A_{0mn}	Coefficients in initial deflection function
AR	Aspect ratio of the plate
a	Plate length
b	Plate breadth
b_f	Stiffener flange breadth
d_w	Uniform reduction in thickness
E	Young modulus of material
h_w	Stiffener web Height
I_n	Neutral moment inertia
m	Number of half-waves in longitudinal direction
n	Number of half-waves in transverse direction
n_y	Number of years of exposure
r_1, r_2	Random numbers corresponding to the corroded surfaces of the plate

S	Standard deviation of random thickness variations
t	Thickness of plate in un-corroded condition
t_{ef}	Effective thickness of plate in corroded condition
t_f	Stiffener flange thickness
t_p	Thickness function of plate in un-corroded condition
t_w	Stiffener web thickness
U_x	Displacement along X-axis
U_y	Displacement along Y-axis
U_z	Displacement along Z-axis
W_0	Initial deflection function
W_{0max}	Maximum magnitude of initial deflection
Z_{UpSRF}	Z-coordinate of the upper surface of the plate
Z_{LowSRF}	Z-coordinate of the lower surface of the plate
ν	Poisson's ratio of material
β	Plate slenderness
μ	Mean corrosion depth
ε	Strain
ε_Y	Material yield strain
σ	Stress
σ_Y	Material yield stress
σ_U	Material ultimate stress
σ_{Ult}	Ultimate strength of the plate

INTRODUCTION

Plates, in either un-stiffened or stiffened configurations, are the most important structural elements of thin-walled structures, such as ship and offshore structures, Figure 1. Ship plates are generally subjected to several types of in-plane or lateral loads. The loads may be applied separately or in combination with each other. Among them, the in-plane loads are almost larger than the other types from the magnitude point of view. The in-plane loads may be tensile or compressive depending on the practical loading conditions. In ship design and also offshore structures, it is essential to ensure that the structure has sufficient strength to sustain extreme loading situations, Figure 2. Strength of plates and stiffened plates are crucial for the overall structural capacity, in other words, for the ultimate strength of the whole structure.

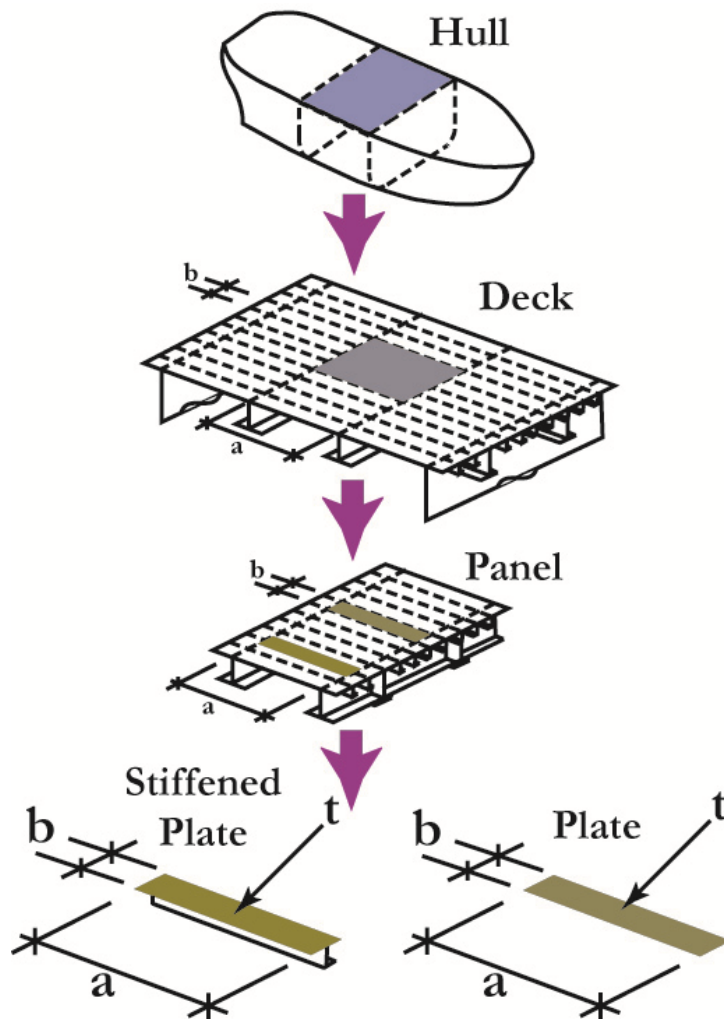


Figure 1: Plate and stiffened plate elements.

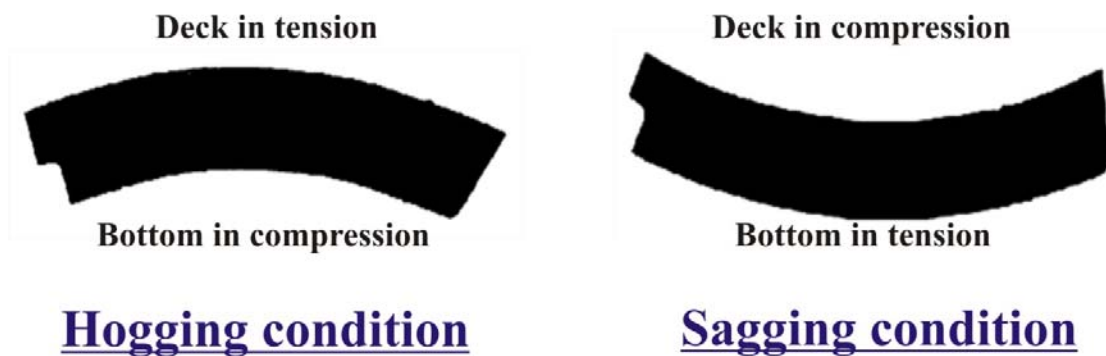


Figure 2: Limit states in hogging or sagging conditions for a ship hull girder.

On the other hand, corrosion and corrosion-related problems are considered to be the most important factors leading to age-related structural degradation of ship and many other types of steel structures. Corrosion has a harmful consequence from the safety point of view and can lead to thickness penetration, fatigue cracks, brittle fracture and unstable failure. These failures can imply a risk of loss of

human lives and a risk of polluting the environment depending on the ship type, as happened in the case of tanker ship "Energy Concentration" (Figure 3) in 1980.

Corrosion in ship structure is mainly observed in two distinct types, namely, general corrosion and localized corrosion. As an example of localized corrosion, reference may be made to the corrosion of hold frames in the way of cargo holds of bulk carriers which have a coating such as tar epoxy paints, Figure 4 [1]. Generally, pitting corrosion is defined as an extremely localized corrosive attack and sites of the corrosive attack are relatively small compared to the overall exposed surface [2]. In the case of localized corrosion observed on hold frames of bulk carriers, the sites of the corrosive attack, i.e. pits, are relatively large (up to about 50mm in diameter).

General corrosion is the problem when the plate elements such as the hold frames of bulk carriers have no protective coating, Figure 5. Both surfaces of the plate may be corroded, in a pattern like the sea waves spectrum, as shown in Figure 5.

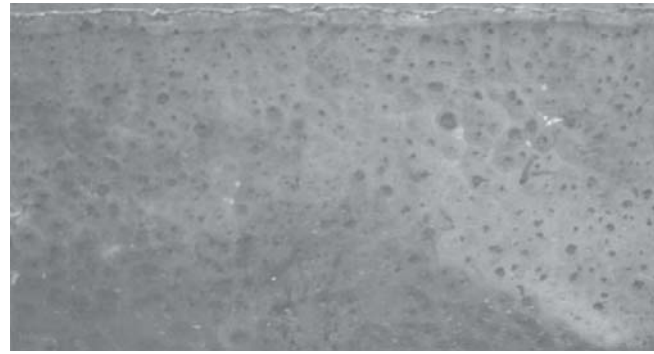


(a)

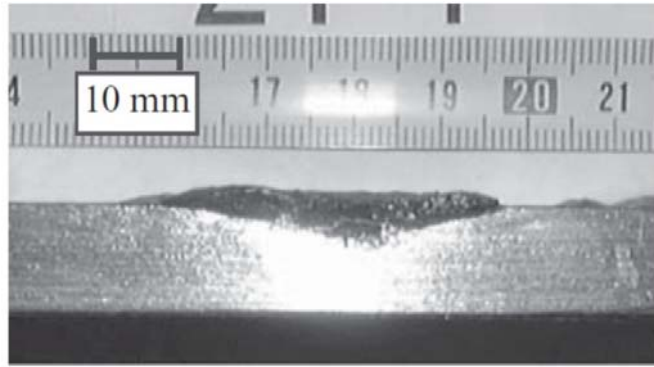


(b)

Figure 3: Collapse of the tanker ship "Energy Concentration": (a) Front view; (b) Longitudinal view.



(a)



(b)

Figure 4: Pitted web plate of the hold frame of a bulk carrier [1]: (a) Pitted surface; (b) Cross-sectional view.



(a)



(b)

Figure 5: Plate with general corrosion: (a) Lower surface; (b) Upper surface.

Mateus and Witz [3] investigated the effect of general corrosion on the post-buckling of plates using the uniform thickness reduction approach and a quasi-random thickness surface model. They revealed that the usual uniform thickness reduction approach to account for general corrosion effects is not adequate because plastic hinges formed due to plate surface irregularity decreases its ultimate strength slightly and affects the post buckling behavior of the plate significantly.

Daidola et al. [4] proposed a mathematical model to estimate the residual thickness of pitted plates using the average and maximum values of pitting data or the number of pits and the depth of the deepest pit, and presented a method to assess the effect of thickness reduction due to pitting on local yielding and plate buckling based on the probabilistic approach. Furthermore, they developed a set of tools which can be used to assess the residual strength of pitted plates.

Slater et al. [5] made a study on the buckling strength and behavior of corroded ship plates using finite element method.

Paik et al. [6,7] studied the ultimate strength characteristics of pitted plate elements under axial compressive loads and in-plane shear loads, and derived closed form formulae for predicting the ultimate strength of pitted plates using the strength reduction (knock-down) factor approach. They dealt with the case where the shape of corrosion pits is a cylinder.

Ok et al. [8] focused on assessing the effects of localized pitting corrosion which concentrates on one or several possibly large area on the ultimate strength of unstiffened plates. They applied multi-variable regression method to derive new formulae to predict ultimate strength of unstiffened plates with localized corrosion. Their results indicated that the length, breadth and depth of pit corrosion have weakening effects on the ultimate strength of the plates while plate slenderness has only marginal effect on strength reduction. It was also revealed that the transverse location of pit corrosion is an important factor determining the amount of strength reduction.

Buckling or ultimate strength of corroded steel plates were investigated experimentally, numerically or analytically by some researchers [9-13]. Most of such studies were performed on the stiffened steel plates with pitted corrosion.

The main objective of the present paper is to examine how general corrosion affects the basic mechanical properties of plate members under compression and to explore the method of simulating behavior of plate members with general corrosion by FE-analysis using shell elements. This paper presents the results of an investigation into the post-buckling behavior and ultimate strength of imperfect corroded steel plates used in ship and other marine-related structures. A series of elastic-plastic large deflection finite element analyses is performed on both-sides randomly corroded steel plates. The effects of general corrosion are introduced into the finite element models using a random thickness surface model. The effects on plate compressive strength as a result of parametric variation of the corroded surface geometry are evaluated. A proposal on the effective thickness is concluded in order to estimate the ultimate strength and explore the post-buckling behavior of randomly corroded steel plates under uniaxial compression. Finally, this research can be used in prediction of aged ships and marine structures ultimate strength, margin of rules safety factor and reliability analysis of them.

FINITE ELEMENT ANALYSIS (FEA)

Extent of the model

The plates in ship and offshore structures are continuous. Longitudinal stiffeners and transverse frames divide the surface of the plates into isolated regions, Figure 6(a). Such regions, which are filled in Figure 6(a), are considered as the model extent in the analyses.

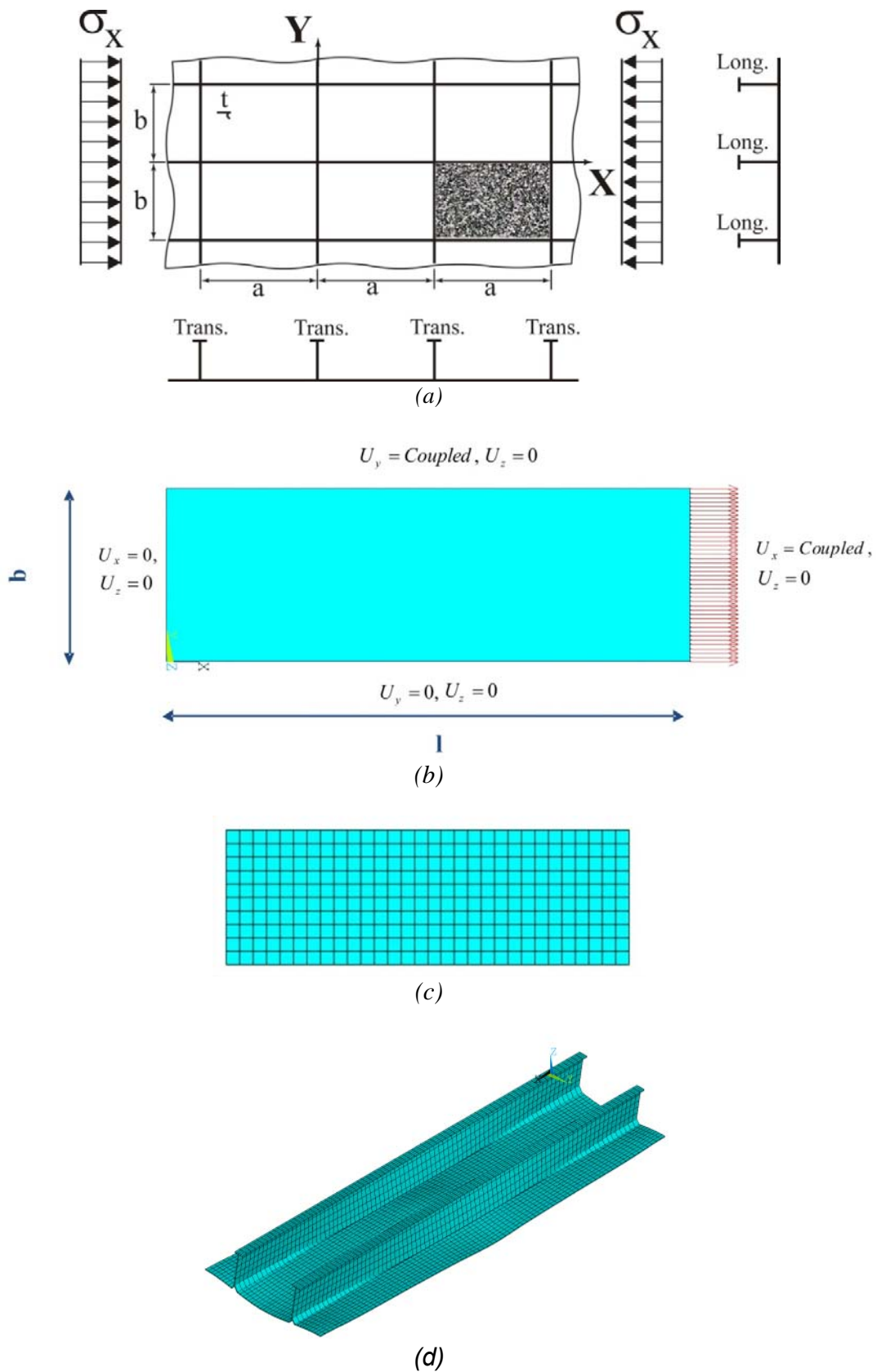


Figure 6: (a) Extent of the model, (b) Boundary and loading conditions (c) Finite element discretization (d) Modeled stiffened plate with scaled initial deflection

Loading and boundary conditions

As shown in Figure 6(a), each region of the continuous plate is isolated by longitudinal stiffeners and transverse frames. To consider the effects of longitudinal stiffeners and transverse frames in the model of isolated plates, proper boundary conditions are to be applied on it. The description of applied boundary condition in the analyses is shown in Figure 6(b). Loading would be compressive along x-axis of the Figure 6(a).

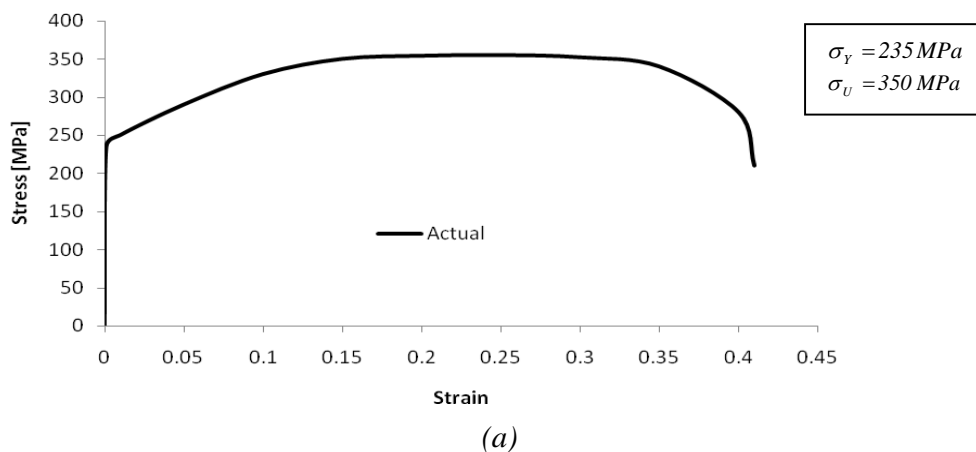
Finite Element code, adopted element and mesh density

The ANSYS powerful software was used in all FE analyses. An APDL code was prepared to facilitate the parametric modeling and analysis using ANSYS [14].

Plates are modeled by SHELL181 elements with elastic-plastic large deflection solution option. SHELL181 is suitable for analyzing thin to moderately-thick shell structures. It is a 4-node element with six degrees of freedom at each node: translations in the x, y, and z directions, and rotations about the x, y, and z-axes. SHELL181 is well-suited for linear, large rotation, and/or large strain nonlinear applications. Changes in shell thickness are accounted for in nonlinear analyses. In order to obtain reasonable results, a number of sensitivity analyses were carried out to find out the optimum mesh density and proper values of nonlinear analysis options. A sample of finite element discretization is represented in Figure 6(c), which is relevant to a plate of aspect ratio equal to 3 with 40 and 20 numbers of mesh divisions in longitudinal and transverse directions, respectively. Element division in web height is 5 and in flange of stiffener is considered 4.

Applied material properties

The material used in the models was of two different types: normal strength steel (abbreviated by NS steel) and high tensile strength steel (abbreviated by HTS steel), Figure 7. Both types of steels have a Young's modulus of 210 MPa and a Poisson's ratio of 0.3. It is evident that strain-hardening effect has some influence on the nonlinear behavior of plates. The degree of such an influence is a function of many factors including plate slenderness. In this study, material behavior for plate was modeled as a bi-linear elastic-plastic manner with strain-hardening rate of $E/65$ Figure 8. This value of strain-hardening rate was obtained through a large number of elastic-plastic large deflection analyses made by Khedmati [15].



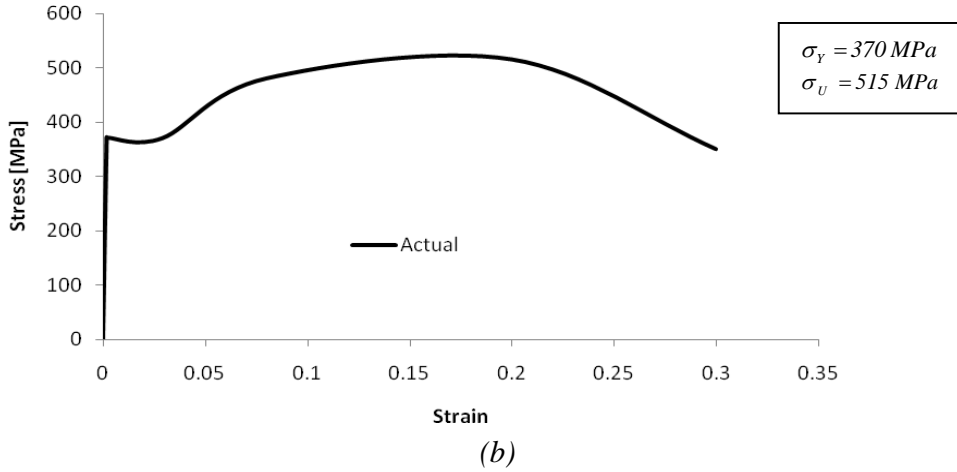


Figure 7: Actual stress-strain curves: (a) NS steel; (b) HTS steel.

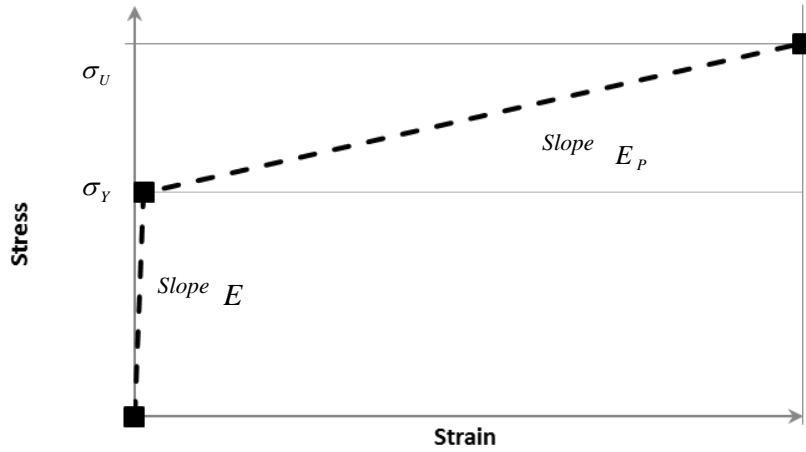


Figure 8: Idealized bilinear model of stress-strain curve for material.

Initial deflection and random general corrosion

The actual mode of the initial deflection of the plate is very complex, Figure 9 [16-17]. This complex mode can be expressed by a double sinusoidal series as:

$$w_0 = \sum_{m=1}^{\infty} \sum_{n=1}^{\infty} A_{0mn} \sin \frac{m\pi x}{a} \sin \frac{n\pi y}{b} \quad (1)$$

When compressive load acts in the direction of the longer side of the plate (x -direction), the deflection components in the direction of the shorter side of the plate (y -direction) decrease with the increase in load except for the first term with one half-wave. In this case, only the first term ($n=1$) may play a dominant role, and the simpler form of the initial deflection can be used for the analysis as follows:

$$w_0 = \sum_{m=1}^{\infty} A_{0m1} \sin \frac{m\pi x}{a} \sin \frac{\pi y}{b} \quad (2)$$

Ueda and Yao [18] used only odd terms. Finally, Yao et. al. [19] introduced even terms also into this mode, and the idealized thin-horse mode took the following form:

$$w_0 = \sum_{m=1}^{11} A_{0m} \sin \frac{m\pi x}{a} \sin \frac{\pi y}{b} \quad (3)$$

The coefficients of this mode are given in Table 1 [19] as functions of plate aspect ratio and its thickness. The maximum magnitude of initial deflection, w_{0max} , is taken as:

$$w_{0max} = 0.05\beta^2 t \quad (4)$$

Where β is the slenderness parameter of the plate and defined by:

$$\beta = \frac{b}{t} \sqrt{\frac{\sigma_Y}{E}} \quad (5)$$

Where σ_Y and E are yield stress and modulus of elasticity of the plate, respectively.

Panel: $a \times b \times t = 2400 \times 800 \times 13.5$

Stiffener: $250 \times 90 \times 9/15$ (in mm)

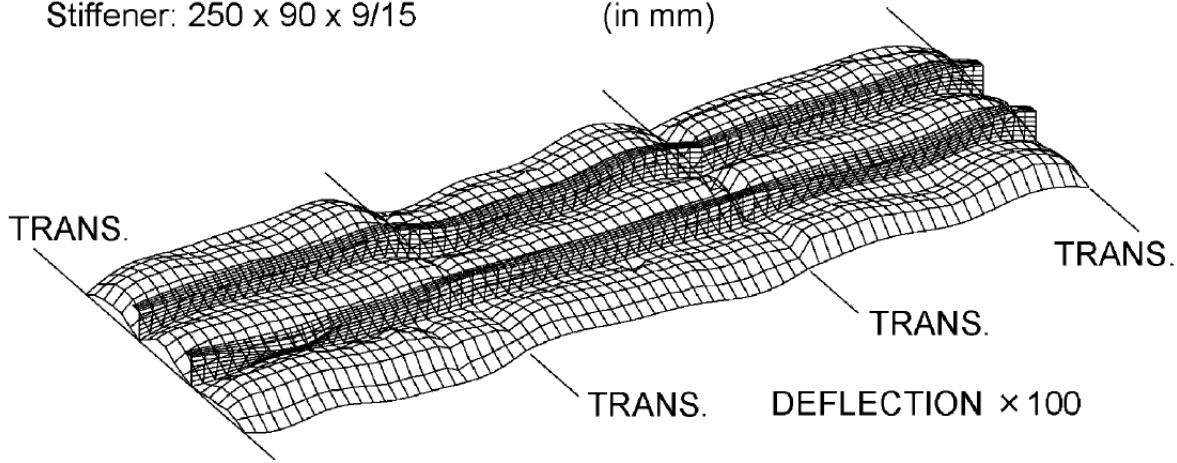


Figure 9: Real distribution of initial deflection or so-called thin-horse mode initial deflection [16-17].

a/b	A_{01}/t	A_{02}/t	A_{03}/t	A_{04}/t	A_{05}/t	A_{06}/t	A_{07}/t	A_{08}/t	A_{09}/t	A_{010}/t	A_{011}/t
$1 < a/b < \sqrt{2}$	1.1158	-0.0276	0.1377	0.0025	-0.0123	-0.0009	-0.0043	0.0008	0.0039	-0.0002	-0.0011
$\sqrt{2} < a/b < \sqrt{6}$	1.1421	-0.0457	0.2284	0.0065	0.0326	-0.0022	-0.0109	0.001	-0.0049	-0.0005	0.0027
$\sqrt{6} < a/b < \sqrt{12}$	1.1458	-0.0616	0.3079	0.0229	0.1146	-0.0065	0.0327	0.000	0.000	-0.0015	-0.0074
$\sqrt{12} < a/b < \sqrt{20}$	1.1439	-0.0677	0.3385	0.0316	0.1579	-0.0149	0.0743	0.0059	0.0293	-0.0012	0.0062
$\sqrt{20} < a/b < \sqrt{30}$	1.1271	-0.0697	0.3483	0.0375	0.1787	-0.0199	0.0995	0.0107	0.0537	-0.0051	0.0256

Table 1: Coefficients of thin-horse mode initial deflection as a function of plate aspect ratio.

Two types of initial imperfection are accounted for stiffeners. Buckling mode initial deflection and angular distortion of the stiffener with the maximum magnitude of

Local plate panels with length, a , of 2400 mm, breadth, b , of 800 mm and thickness, t , 13 mm with different stiffener type and dimensions are considered. The considered stiffeners properties are shown in table 2.

Type	Model	Shape	h_w	t_w	b_f	t_f	$I_n [cm^4]$
1	F1	Flat	150	17	-	-	4,781
1	T1	tee	150	9	90	12	5,233
1	A1	angle	150	9	90	12	5,233
2	F2	Flat	250	19	-	-	24,739
2	T2	tee	250	10	90	15	24,240
2	A2	angle	250	10	90	15	24,240
3	F3	Flat	350	35	-	-	125,052
3	T3	tee	400	12	100	17	105,900
3	A3	angle	400	12	100	17	105,900

Table 2: Stiffeners Properties

A plate subject to general corrosion has a random distribution of thickness over its area. The likelihood of these variations in thickness to form plastic hinges that may affect the buckling and post-buckling behavior of a corroded plate, and perhaps its ultimate strength, is something that cannot be discarded without further analysis. Creation of plastic hinge affects buckling (except elastic buckling) and post buckling behavior.

It may be reasonable to assume that the corroded surfaces of a plate with its random thickness variation is composed of an infinite summation of random coefficients associated with each of the elastic buckling modes of the plate. Melchers (1994) used data collected from unpainted steel plate and presented as below [24]:

$$d_{wgs} = \begin{cases} 0.200n & , 0 \leq n < 1.3 \\ 0.130 + 0.100n & , 1.3 \leq n < 16 \end{cases}$$

Where n is the time of exposure in years, and d_w is the uniform reduction in thickness (or corrosion depth), due to corrosion effects, after n years of exposure.

In numerical terms, the general corrosion model describes the typical surfaces of a corroded plate as a random thickness variation, t_p , with an average value equal to the original thickness of plate, minus the corroded equivalent thickness reduction. The following expression was applied in the studies made by Mateus and Witz [3]:

$$t_p(x, y) = t - d_w + \sum_{i=1}^{\infty} \sum_{k=1}^{\infty} (A_i \cdot f_i(x) + B_k \cdot g_k(y)) \quad (6)$$

Where A_i and B_k are the random coefficients associated with mode i in the x -direction and the mode k in the y -direction, respectively, and $f_i = \sin(i\pi x/a)$, $g_k = \sin(k\pi y/b)$. In this paper, randomly corroded surfaces were generated for both sides of the plate, instead of above-mentioned expression of double sinusoidal summation. A special purpose computer code was written in FORTRAN90 language. The generation of randomly corroded thicknesses was achieved using the features of the DRANDM function of FORTRAN90. Finally, the z -coordinate of upper and lower surfaces of the plate can be defined as in Figure 10(a)

$$z_{LowSRF} = w_0 - \frac{t-d_w}{2} - r_1, \quad z_{UpSRF} = w_0 + \frac{t-d_w}{2} + r_2 \quad (7)$$

Where

$$t_p = z_{UpSRF} - z_{LowSRF} = t - d_w + r_1 + r_2 \quad (8)$$

And also, r_1 and r_2 are the random numbers, corresponding to the random thickness variation of the plate surfaces, produced by DRANDM function.

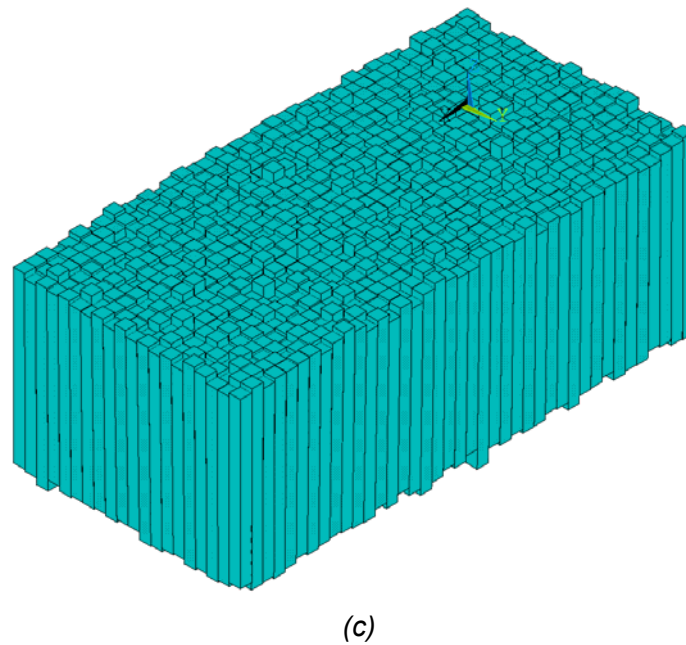
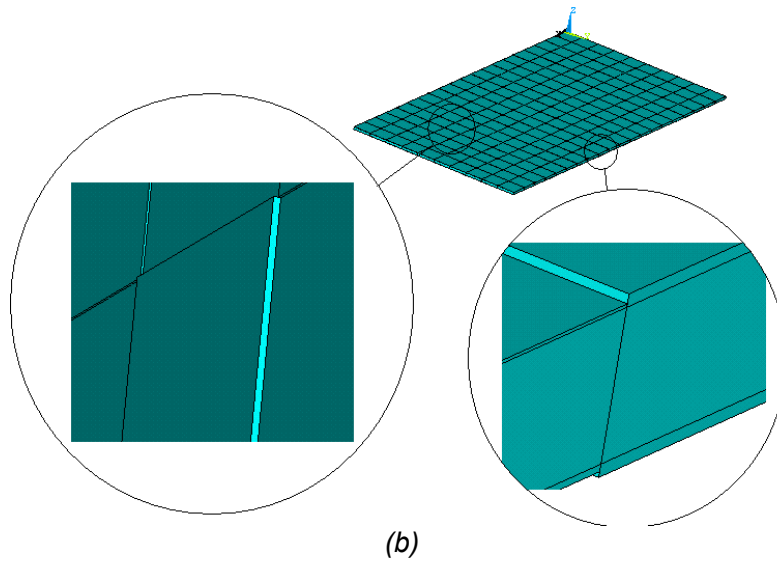
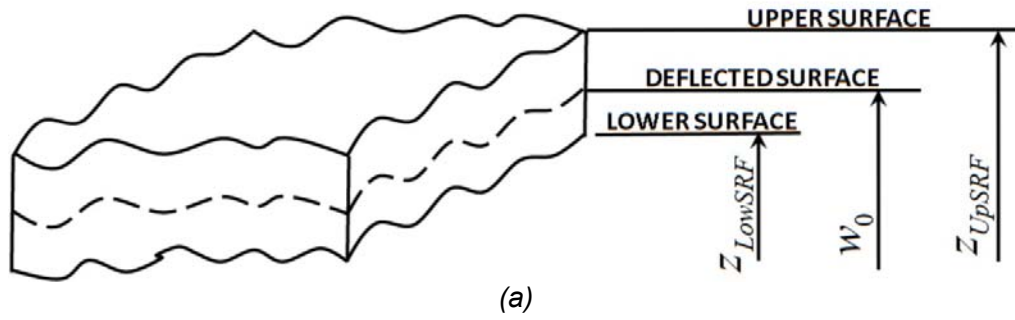


Figure 10: Finite element analysis modeling details for general corrosion: (a) Different surfaces and relevant parameters; (b) Plate discretization; (c) Perspective view of the randomly corroded plate with magnified thickness.

There are several finite element techniques available to model uniform corrosion. The easiest way is to reduce the thickness of the plate in surface, to carry out buckling analysis to get the buckled shape of plate with uniform corrosion and finally to perform nonlinear finite element control to get the ultimate strength of plate by using stress versus strain relationship. Khedmati and Karimi [21] modeled the corroded plate with 3-D 20-node structural solid element but this method also cannot represent the real situation and easily tends to fail to converge during nonlinear control according to the author's experience.

Figure 10(b) represents the modeling details in finite element analysis while Figure 10(c) shows a magnified view of the plate with surfaces simulating random corrosion.

Validation

Various unstiffened and stiffened plate models in uncorroded condition have been tested experimentally by Ghavami [22]. Some of these models were successfully simulated by Ghavami and Khedmati [23]. The obtained experimental and numerical results showed a very good agreement. Upon such successful agreements, numerical simulations are extended here on the corroded models.

PARAMETRIC STUDY

In order to study the effects of random thickness variation on the response of axially loaded plates, different cases were considered. The cases included in the study are briefly explained as follows:

- Corroded plates with $AR=2$, $t=14$ mm, mean corrosion depth=2mm and $S=0.2$ made of HTS steel
- Corroded plates with $AR=3$, $t=14$ mm, mean corrosion depth=2mm and $S=0.2$ made of HTS steel
- Corroded plates with $AR=2$, $t=18$ mm, mean corrosion depth=2mm and $S=0.2$ made of HTS steel
- Corroded plates with $AR=3$, $t=18$ mm, mean corrosion depth=2mm and $S=0.2$ made of HTS steel
- Corroded plates with $AR=2$, $t=14$ mm, mean corrosion depth=2mm and $S=0.2$ made of NS steel
- Corroded plates with $AR=3$, $t=14$ mm, mean corrosion depth=2mm and $S=0.2$ made of NS steel
- Corroded plates with $AR=2$, $t=18$ mm, mean corrosion depth=2mm and $S=0.2$ made of NS steel
- Corroded plates with $AR=3$, $t=18$ mm, mean corrosion depth=2mm and $S=0.2$ made of NS steel

For each of the above cases, 50 models were created changing the random thickness variation parameters. The corroded surfaces of the models were different in these cases. Gaussian distribution for random thickness variation was considered in all cases and corresponding models. All of the plate models were analyzed under longitudinal in-plane compression. Average stress-average strain relationships for the models are shown in Figures. 11, 12, 13, 14, 15, 16, 17 and 18, respectively. The maximum magnitude of thin-horse mode initial deflection for the corroded models is calculated using Eq. 4 for the original thickness. Also, Von Mises stress distributions are shown for a selection of the cases in Tables 3, 4, 5, 6 and 7. Sample perspective views on the surfaces of a plate with random Gaussian distribution of corrosion are shown in Figure 19.

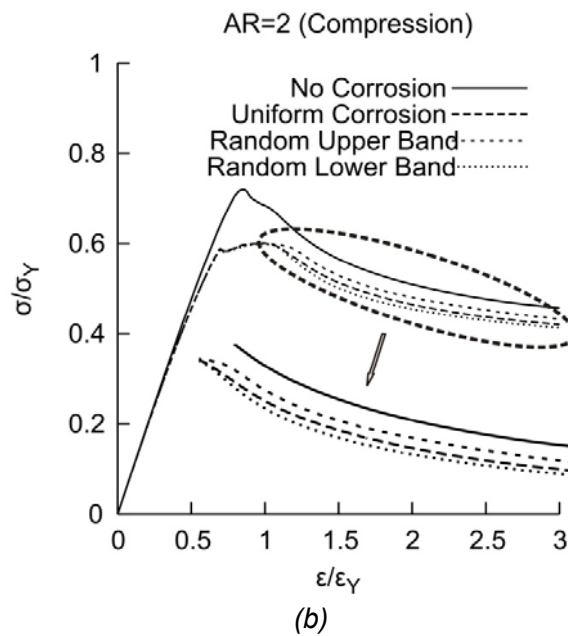
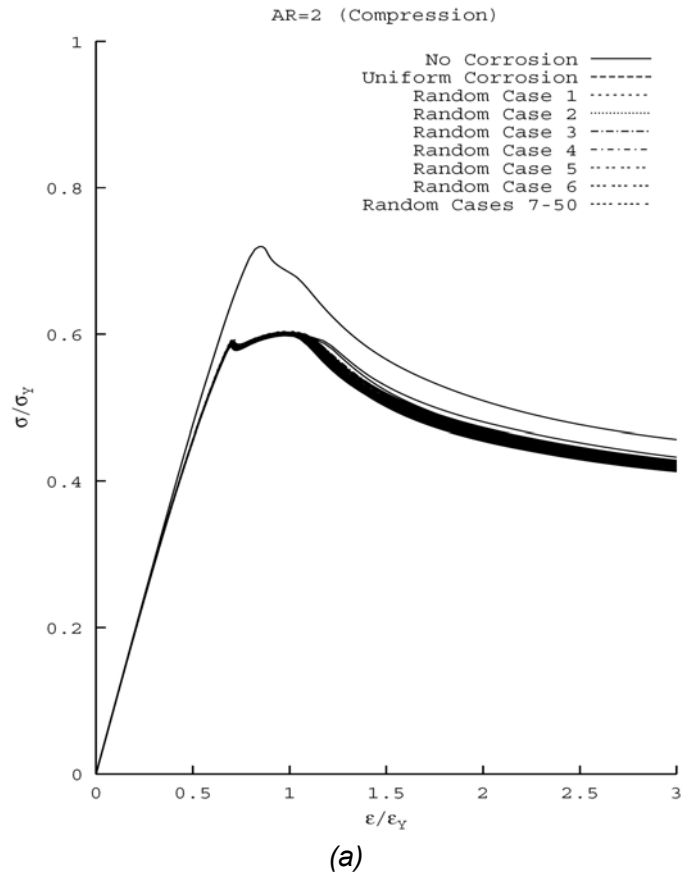


Figure 11: Comparison of average stress-average strain relationships for corroded plates with AR=2, $t=14$ mm, mean corrosion depth=2mm and $S=0.2$ made of HTS steel.

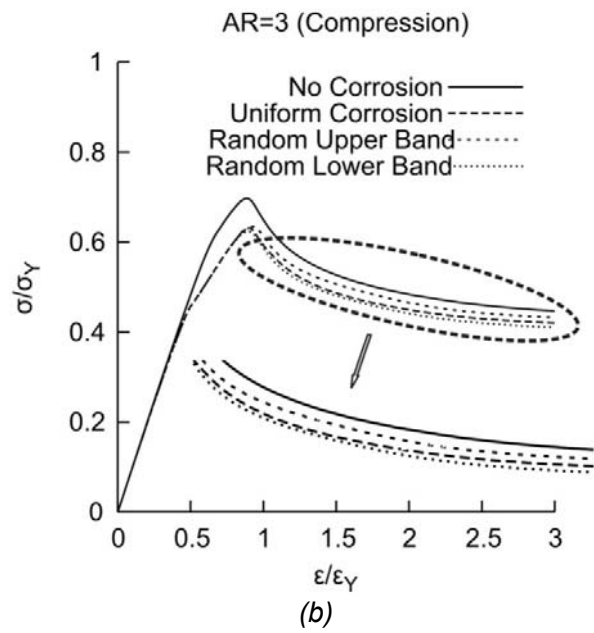
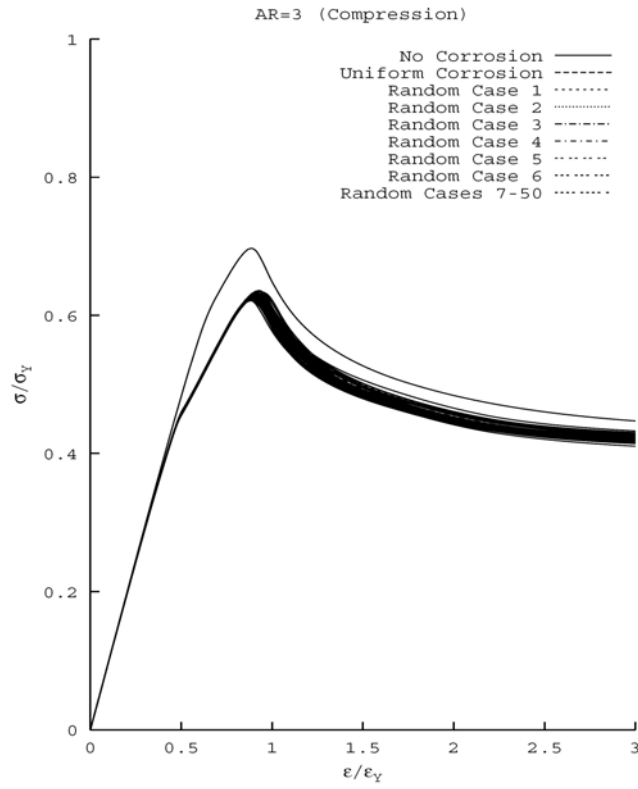


Figure 12: Comparison of average stress-average strain relationships for corroded plates with AR=3, $t=14$ mm, mean corrosion depth=2mm and $S=0.2$ made of HTS steel.

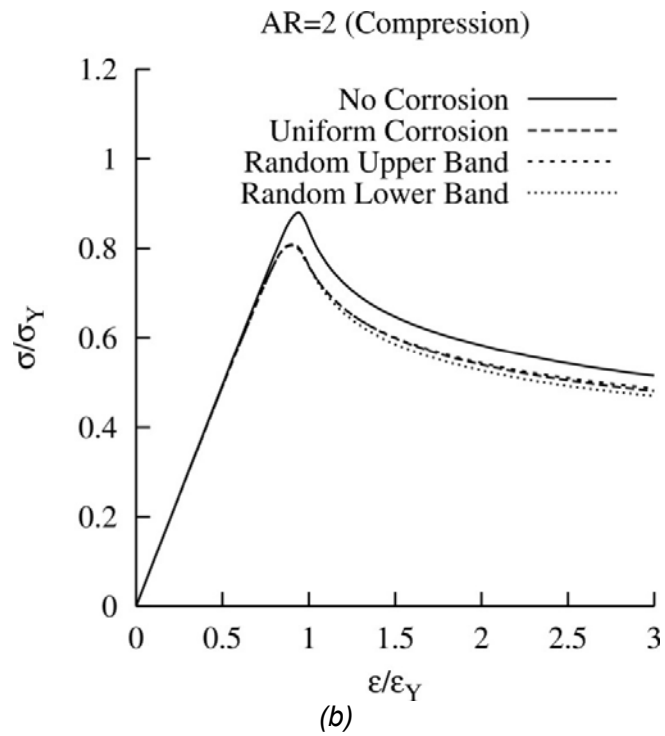
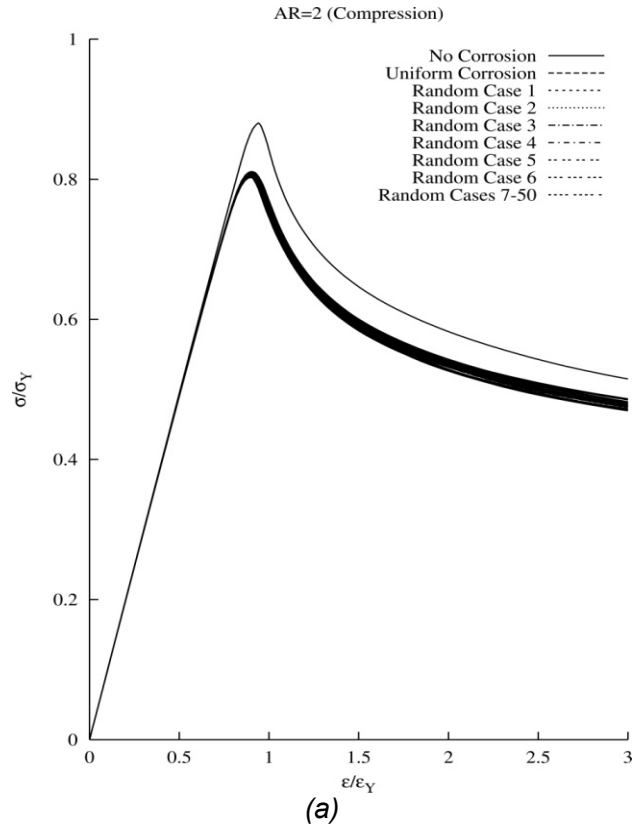


Figure 13: Comparison of average stress-average strain relationships for corroded plates with AR=2, $t=18$ mm, mean corrosion depth=2mm and $S=0.2$ made of HTS steel.

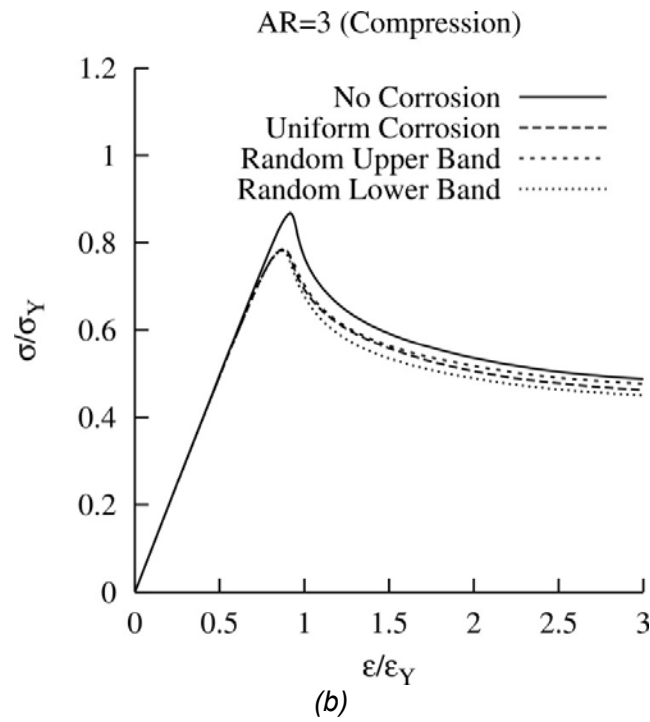
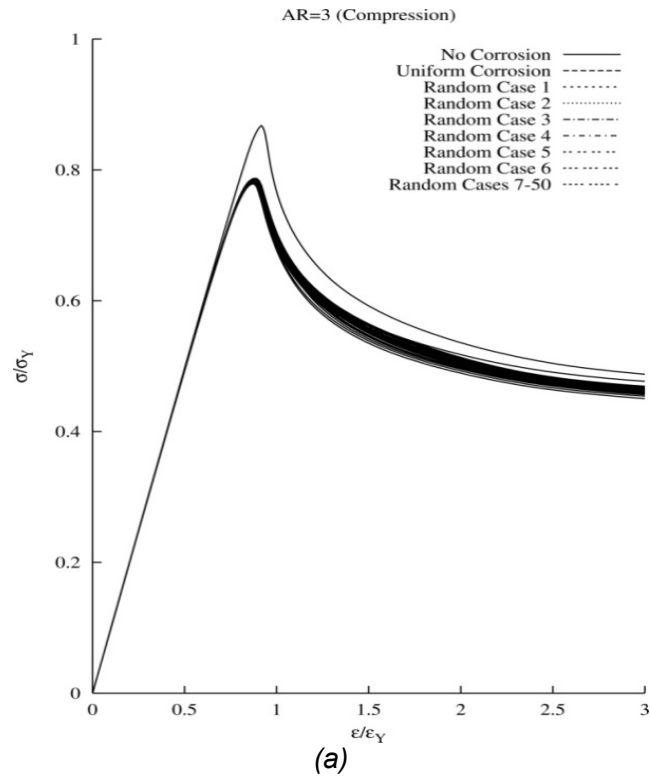


Figure 14: Comparison of average stress-average strain relationships for corroded plates with AR=3, $t=18$ mm, mean corrosion depth=2mm and $S=0.2$ made of HTS steel.

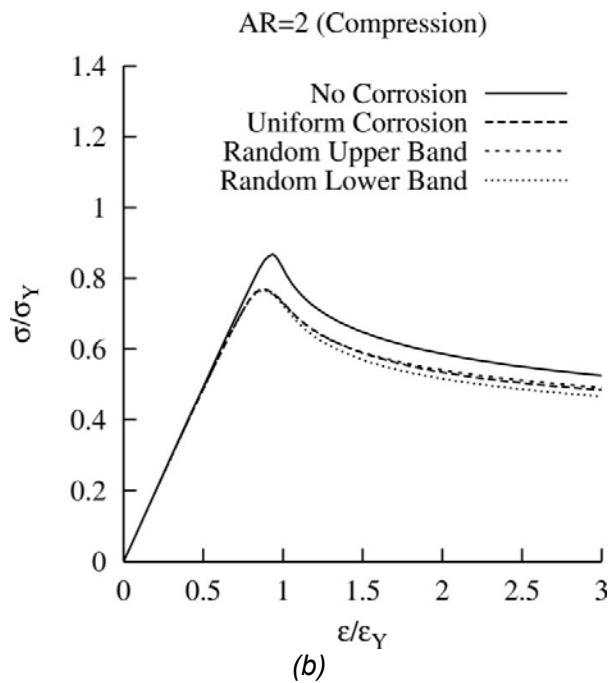
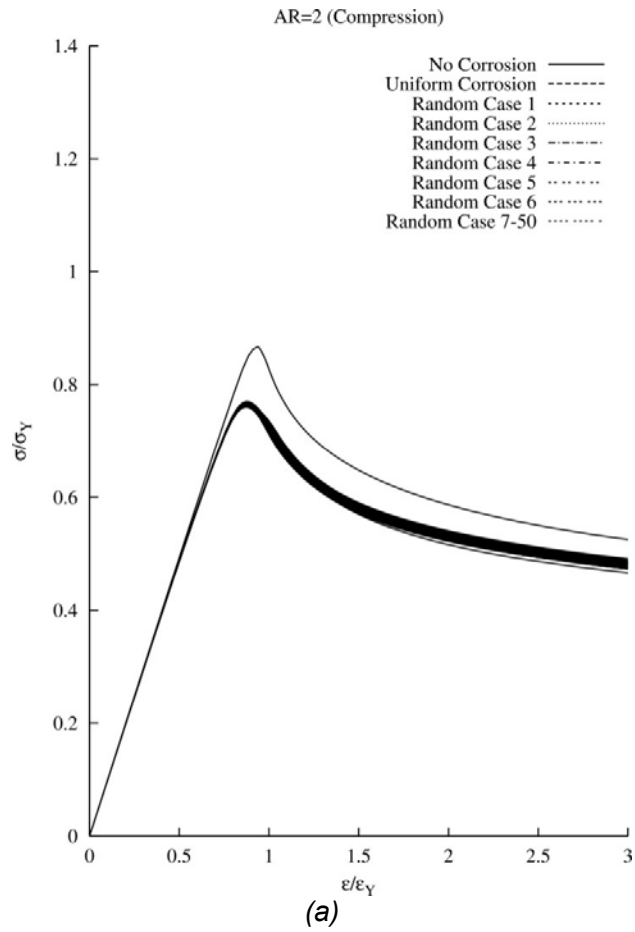


Figure 15: Comparison of average stress-average strain relationships for corroded plates with AR=2, $t=14$ mm, mean corrosion depth=2mm and $S=0.2$ made of NS steel.

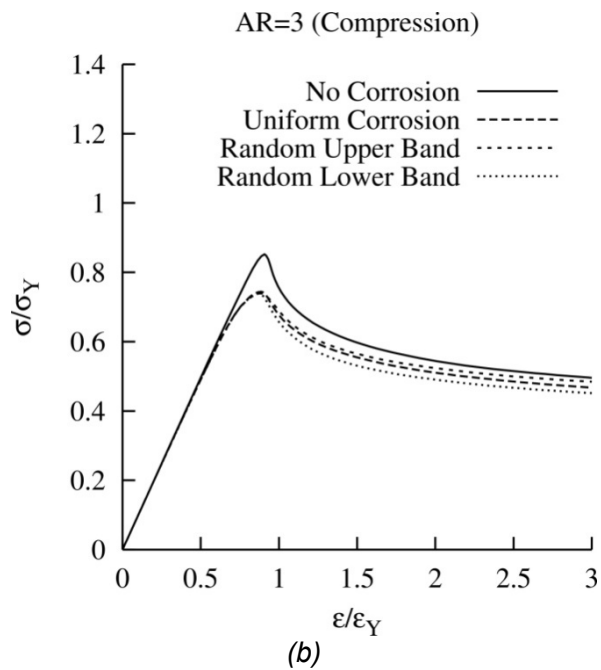
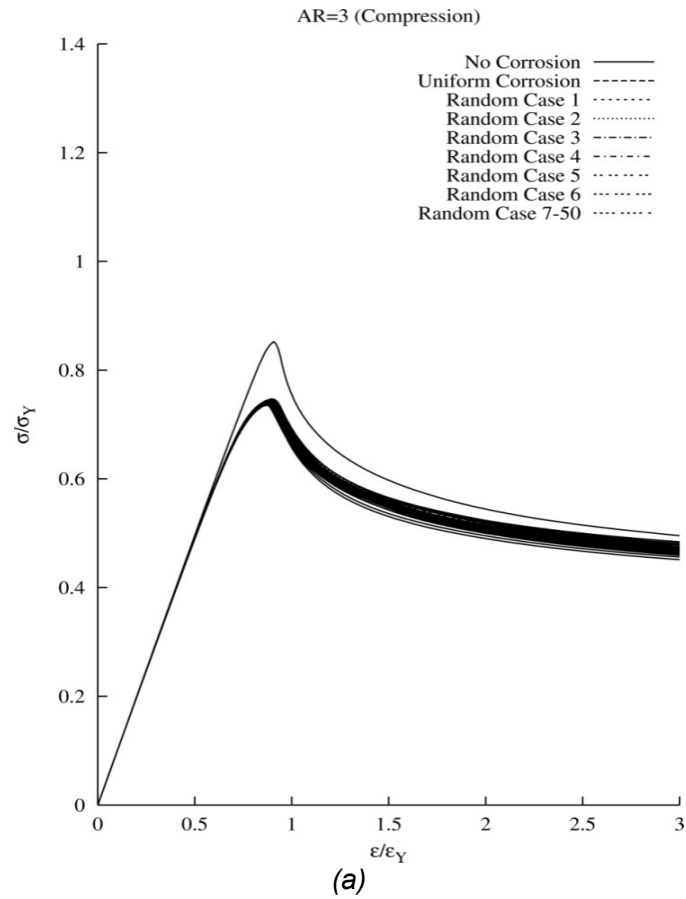


Figure 16: Comparison of average stress-average strain relationships for corroded plates with AR=3, $t=14$ mm, mean corrosion depth=2mm and $S=0.2$ made of NS steel.

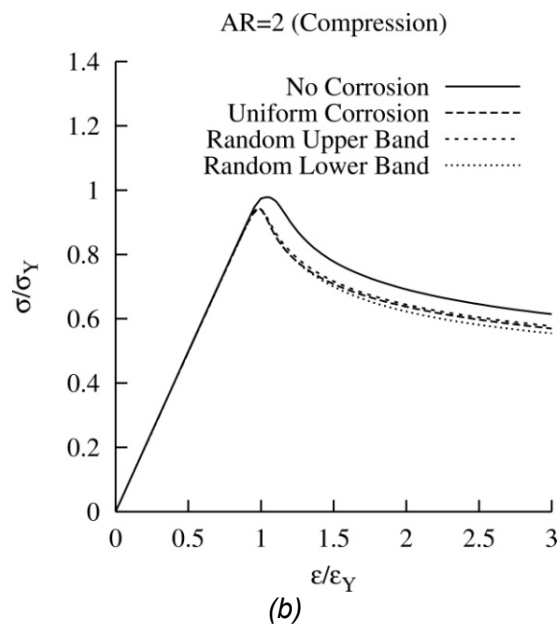
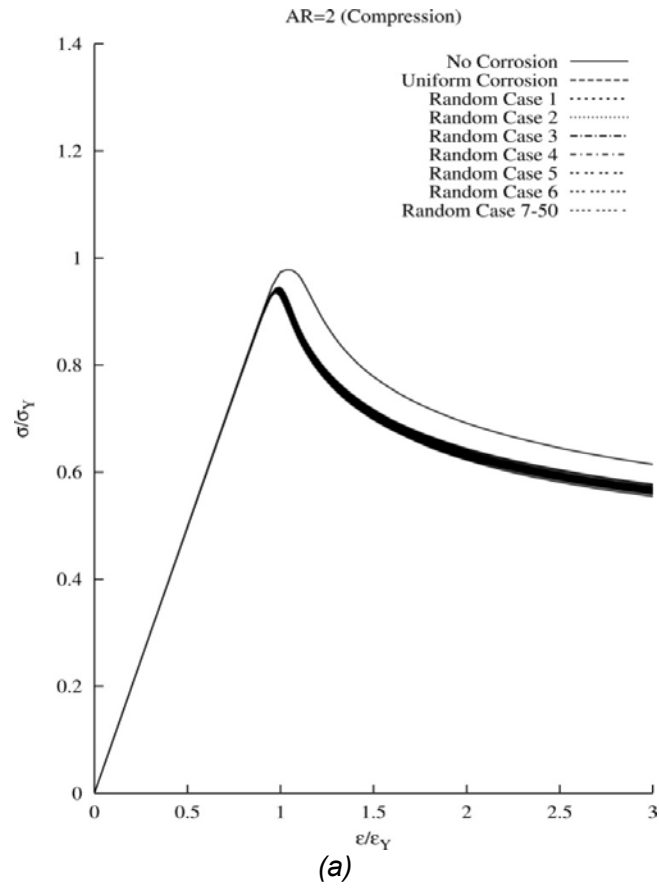


Figure 17: Comparison of average stress-average strain relationships for corroded plates with AR=2, $t=18$ mm, mean corrosion depth=2mm and $S=0.2$ made of NS steel.

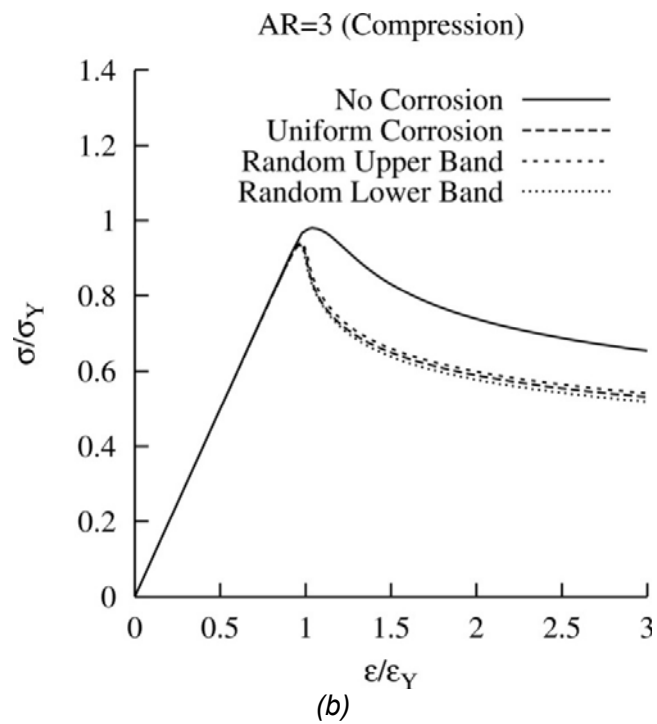
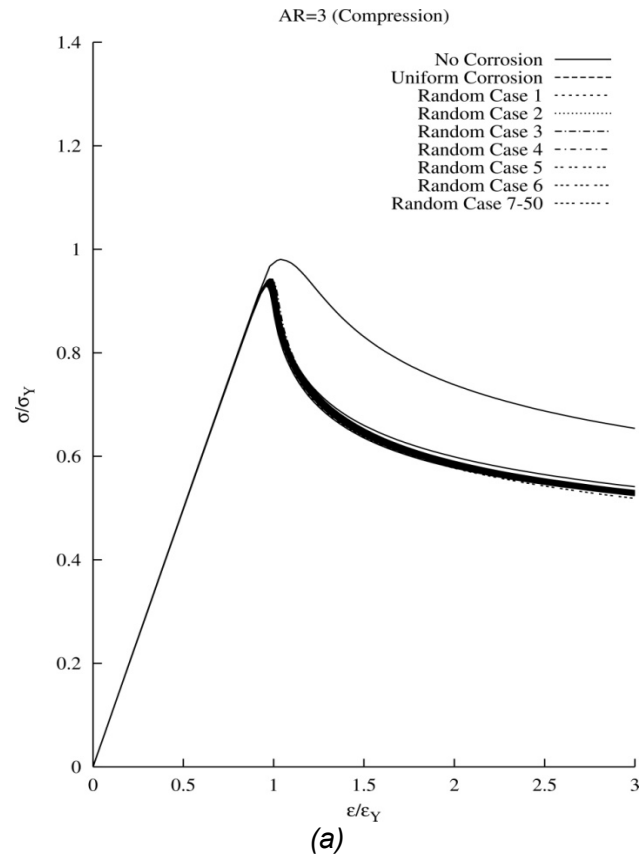
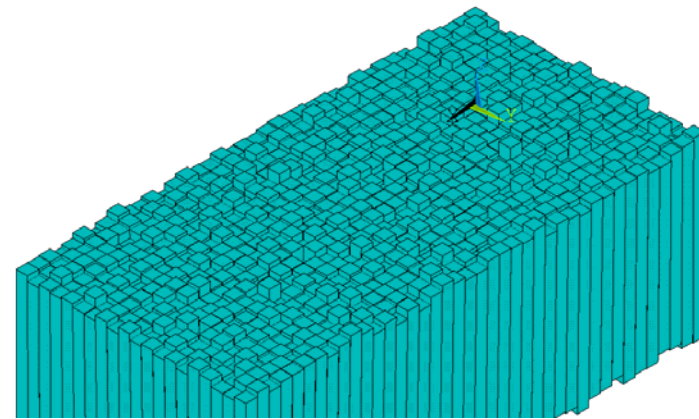
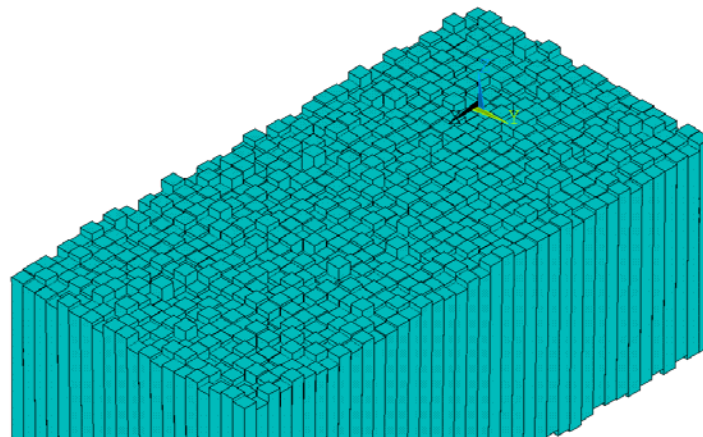


Figure 18: Comparison of average stress-average strain relationships for corroded plates with AR=3, $t=18$ mm, mean corrosion depth=2mm and $S=0.2$ made of NS steel.



(a)



(b)

Figure 19: Perspective views on the surfaces of the plate with random Gaussian distribution of corrosion ($AR=2$, $t=14$ mm, mean corrosion depth=2mm, $S=0.2$ and made of HTS steel): (a) Lower band; (b) Upper band.

The average stress-average strain relationships of the plate models in un-corroded condition as well as in the condition of having uniform thickness reduction are shown in Figs 11 to 18. The plate in the condition of uniform corrosion or uniform thickness reduction has a reduction equal to the mean corrosion depth from its original un-corroded thickness.

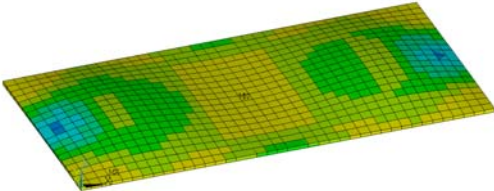
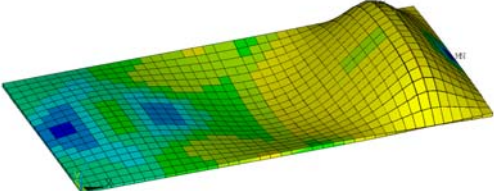
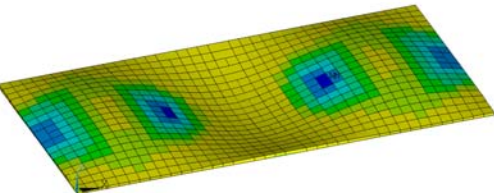
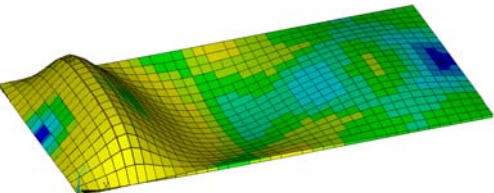
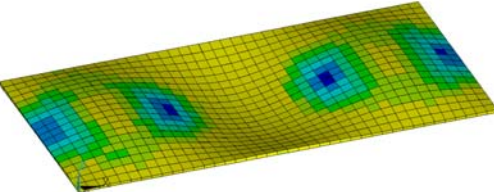
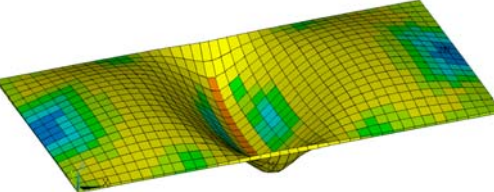
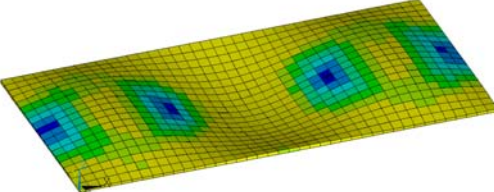
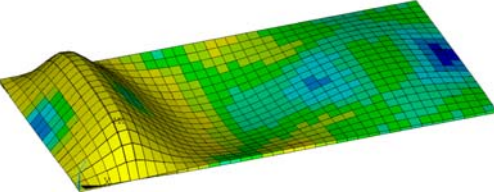
Figures 11 to 18 in addition to the results summarized in Tables 3 to 7 reveal the following main characteristics for the buckling/ultimate strengths and behaviors of the corroded plate models

- Random thickness variations in the plate model surfaces mainly affect their post-ultimate-strength regimes while their pre-ultimate-strength behaviours are almost unchanged.
- Random thickness variation scheme applied to the plate surfaces has led to a reduction in the buckling and ultimate strengths of the models. The amount of reduction is a function of plate aspect ratio, plate thickness (slenderness parameter) and also the plate material.
- The difference between the buckling strengths of corroded plate models with that of their corresponding un-corroded condition is in the ranges of 17-37 percent and 4-18 percent in cases of using HTS or NS steels, respectively.
- Besides, the difference between the ultimate strengths of corroded plate models with that of their corresponding un-corroded condition is in the ranges of 5-26 percent without any specific trend. The main parameter influencing this reduction seems to be the plate slenderness parameter or thickness. The thicker the plate, the less the reduction in the ultimate strength of the corroded plate model in comparison with its corresponding un-corroded condition.

- The curve of average stress-average strain for the condition of uniformly corroded plate model lies inside the band of average stress-average strain relationships of corresponding randomly corroded models. This can be well understood by paying attention to Figs. 11(b) to 18(b) where the curve of uniformly corroded plate model is seen to be in between the curves, corresponding to upper and lower limits of the bands in each of the analysed cases. In other words, the curve of the uniformly corroded plate model may be regarded as the practical mean curve representing the average stress-average strain relationship of the randomly corroded plate models in each case.

- The mode shapes and Von Mises stress contours shown in Tables 3 to 7 reveal that almost regular half-waves are generated inside the plate extent in longitudinal direction at the ultimate strength level. Besides, post-ultimate-strength mode shapes show the local accumulation of deflection in some regions of the plate model in addition to the unloading the rest of plate area. The place of local deflection accumulation is not fixed and, in other words, changes from case to case.

Plate $2400 \times 800 \times 14$, $W_{0max} = 0.05\beta^2t$, 2mm Corrosion

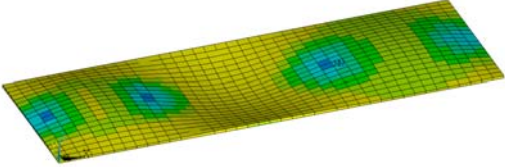
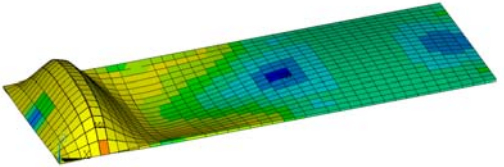
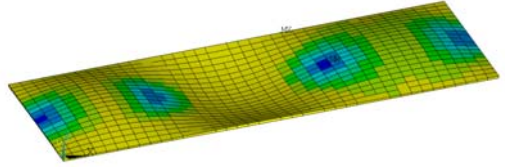
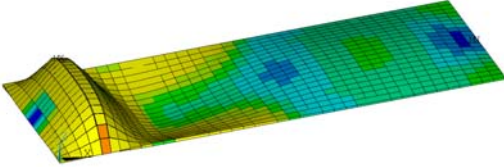
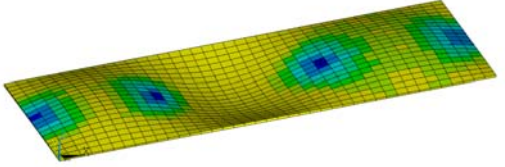
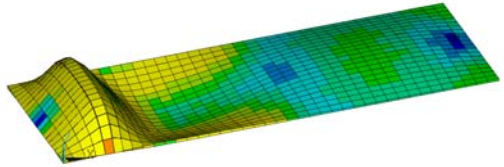
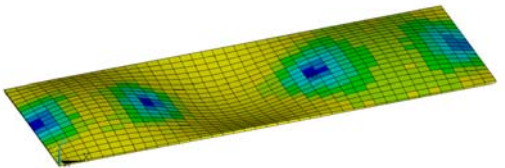
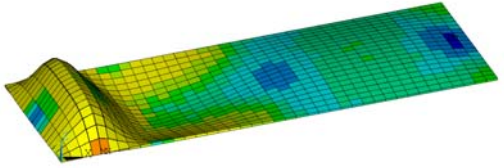
Case	Ultimate strength step	$\frac{\sigma_{ave}}{\sigma_V}$	Final Step $\frac{\epsilon}{\epsilon_Y} = 3$	$\frac{\sigma_{ave}}{\sigma_V}$
No Corrosion		0.720		0.457
Uniform Corrosion		0.600		0.418
Random Upper Band		0.601		0.431
Random Lower Band		0.599		0.412

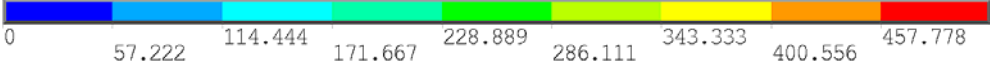


0 57.222 114.444 171.667 228.889 286.111 343.333 400.556 457.778 515

Table 3: Von-Mises stress contours for 14 mm plate models of aspect ratio of 2, made of HTS steel.

Plate $2400 \times 800 \times 14, W_{0max} = 0.05\beta^2t, 2mm$ Corrosion

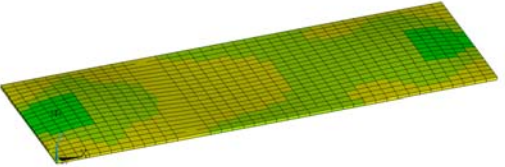
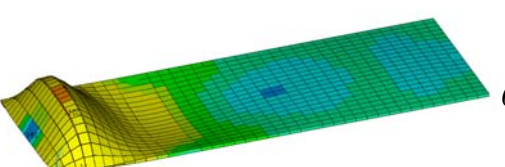
<i>Case</i>	<i>Ultimate strength step</i>	$\frac{\sigma_{ave}}{\sigma_Y}$	<i>Final Step $\frac{\epsilon}{\epsilon_Y} = 3$</i>	$\frac{\sigma_{ave}}{\sigma_Y}$
<i>No Corrosion</i>		0.697		0.447
<i>Uniform Corrosion</i>		0.631		0.420
<i>Random Upper Band</i>		0.634		0.432
<i>Random Lower Band</i>		0.624		0.410



0 57.222 114.444 171.667 228.889 286.111 343.333 400.556 457.778 515

Table 4: Von-Mises stress contours for 14 mm plate models of aspect ratio of 3, made of HTS steel.

Plate $2400 \times 800 \times 18, W_{0max} = 0.05\beta^2t, 2mm$ Corrosion

<i>Case</i>	<i>Ultimate strength step</i>	$\frac{\sigma_{ave}}{\sigma_Y}$	<i>Final Step $\frac{\epsilon}{\epsilon_Y} = 3$</i>	$\frac{\sigma_{ave}}{\sigma_Y}$
<i>No Corrosion</i>		0.868		0.488

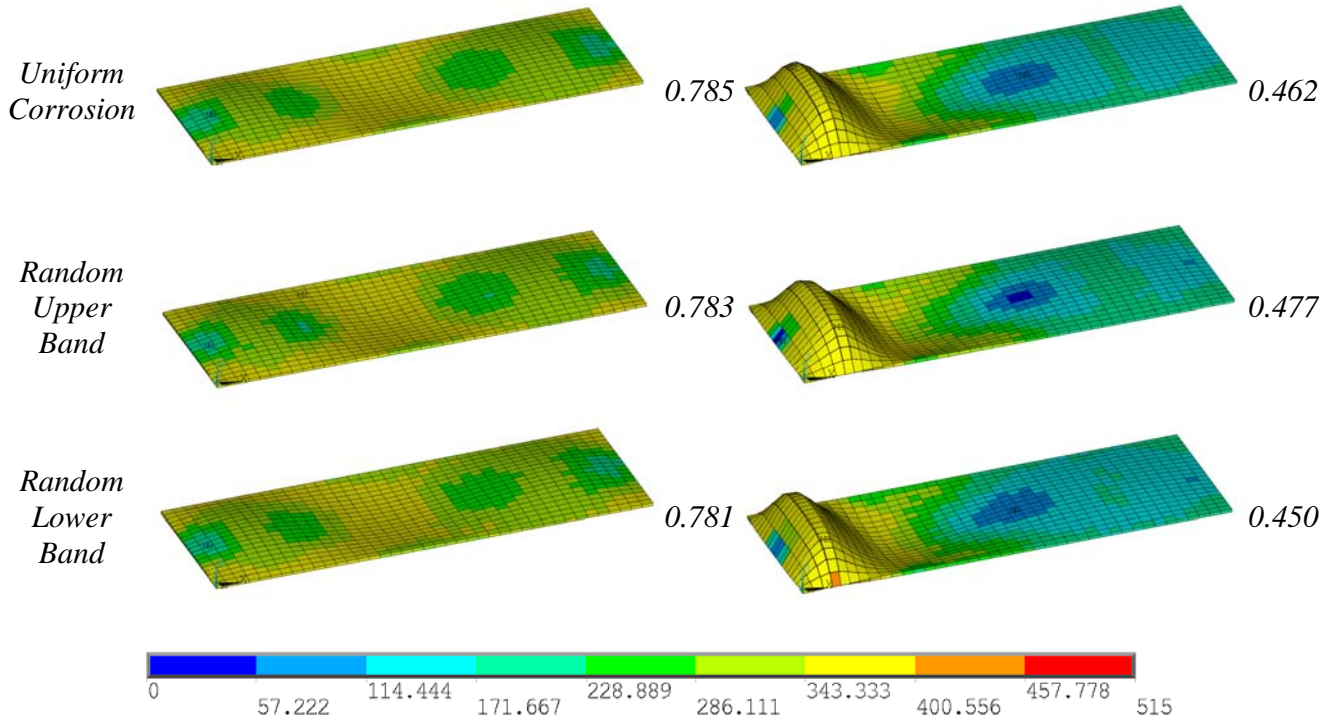


Table 5: Von-Mises stress contours for 18 mm plate models of aspect ratio of 3, made of HTS steel.

Plate $2400 \times 800 \times 14$, $W_{0max} = 0.05\beta^2t$, 2mm Corrosion

Case	Ultimate strength step	$\frac{\sigma_{ave}}{\sigma_Y}$	Final Step $\frac{\varepsilon}{\varepsilon_Y} = 3$	$\frac{\sigma_{ave}}{\sigma_Y}$
No Corrosion		0.852		0.494
Uniform Corrosion		0.744		0.466
Random Upper Band		0.779		0.483

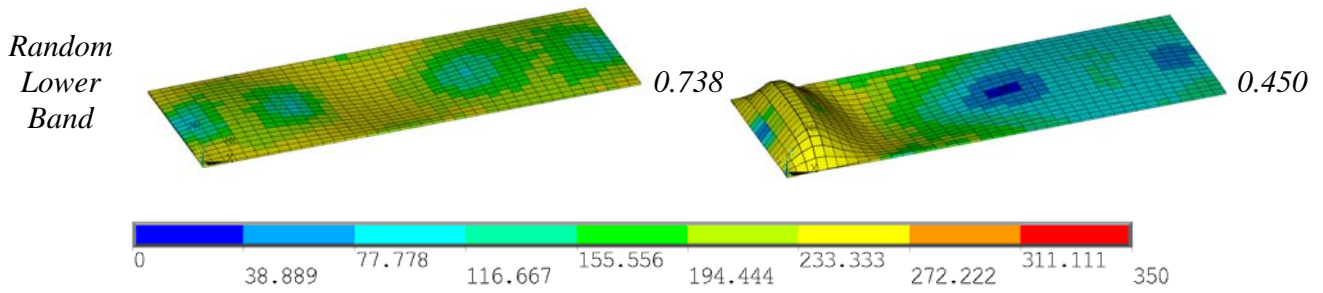


Table 6: Von-Mises stress contours for 14 mm plate models of aspect ratio of 3, made of NS steel.

Plate $2400 \times 800 \times 18$, $W_{0max} = 0.05\beta^2t$, 2mm Corrosion

Case	Ultimate strength step	$\frac{\sigma_{ave}}{\sigma_Y}$	Final Step $\frac{\epsilon}{\epsilon_Y} = 3$	$\frac{\sigma_{ave}}{\sigma_Y}$
No Corrosion		0.981		0.652
Uniform Corrosion		0.939		0.529
Random Upper Band		0.939		0.539
Random Lower Band		0.935		0.517

Table 7: Von-Mises stress contours for 18 mm plate models of aspect ratio of 3, made of NS steel.

PROPOSAL ON EFFECTIVE THICKNESS

Based on the results given in Figs. 11 to 18 and above-mentioned descriptions, the following equation is proposed as the effective thickness of the plate having random corrosion, for practical evaluation of its average stress-average strain relationship and strength characteristics

$$t_{ef} = t - \mu - S \quad (10)$$

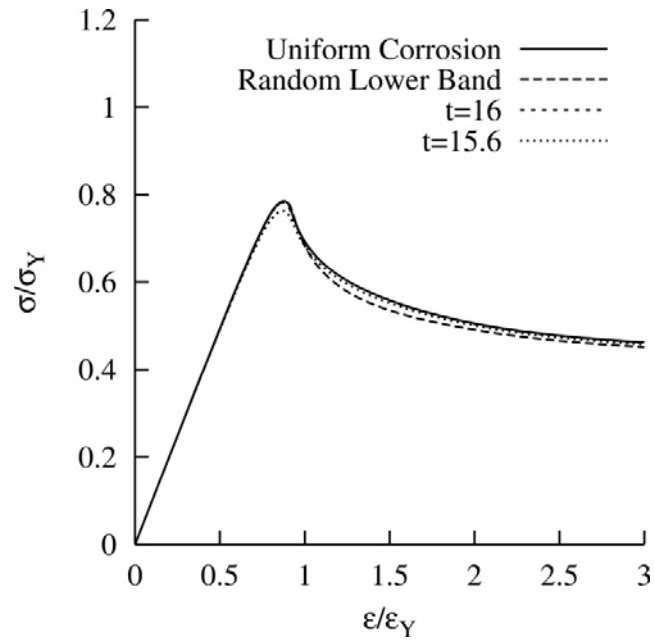
Figures 20(a) and 20(b) give some explanations for the usefulness of applying the above equation. The plate under consideration in these figures has a length of 2400 mm, breadth of 800 mm, original un-corroded thickness of 18 mm and is made of HTS steel. It is assumed that the plate has a random Gaussian distribution of corrosion on its both surfaces. The mean corrosion depth is assumed to be either 2 mm (Fig. 20(a)) or 4 mm (Fig. 20(b)). Standard deviation of the Gaussian distribution of random thickness is set to 0.4. Four average stress-average strain curves are seen in either Fig 20(a) or 20(b). The description of these four curves is as follows:

- **Solid line:** corresponding to the plate with uniform corrosion. This means that the plate has a thickness equal to its original thickness (18 mm) minus mean corrosion depth. The maximum magnitude of thin-horse mode initial deflection is calculated using Eq. 4 for the original thickness (18 mm).
- **Dashed line:** corresponding to the lower band or limit curve for the plate with random Gaussian distribution of corrosion. The maximum magnitude of thin-horse mode initial deflection is calculated using Eq. 4 for the original thickness (18 mm).
- **Short-dashed line:** corresponding to the plate with uniform corrosion. This means that the plate has a thickness equal to its original thickness (18 mm) minus mean corrosion depth. The maximum magnitude of thin-horse mode initial deflection is calculated using Eq. 4 for the uniformly corroded thickness.
- **Dotted line:** corresponding to the plate with equivalent or effective thickness. The maximum magnitude of thin-horse mode initial deflection is calculated using Eq. 4 for the effective thickness.

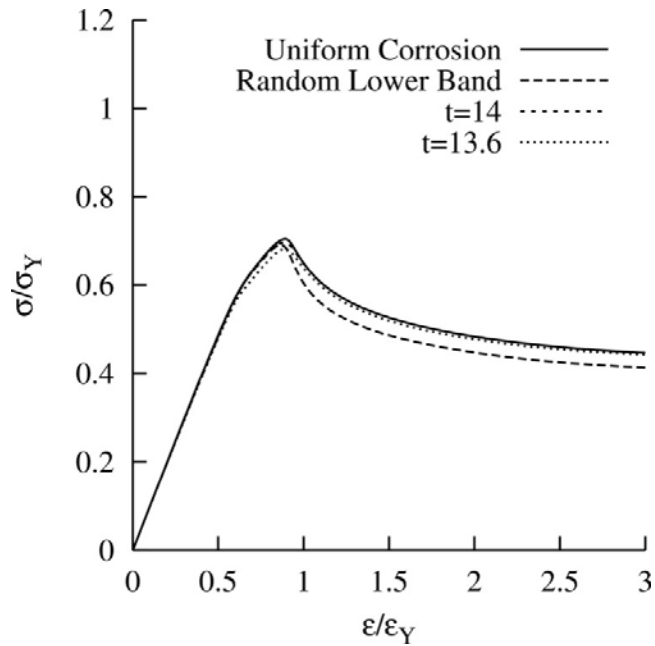
As can be seen from Figs. 20(a) and 20(b), the average stress-average strain relationship derived using the effective thickness (based on Eq. 10) agrees well with that obtained for the other cases. Also, applying the effective thickness proposal in Eq. 10, the ultimate strength of the randomly corroded plate can be easily estimated based on the following set of equations [24]

$$\frac{\sigma_{ult}}{\sigma_f} = \begin{cases} 1.0 & \text{for } \beta \leq 1.73 \\ 0.1 + \frac{1.871}{\beta} & \text{for } \beta > 1.73 \end{cases} \quad (11)$$

Where β is to be calculated using the effective thickness of the corroded plate.



(a)



(b)

Figure 20: Comparison of average stress-average strain relationships for a plate with random Gaussian distribution of corrosion ($a=2400$ mm, $b=800$ mm, $t=18$ mm, mean corrosion depth=2 and 4 mm, $S=0.4$ and made of HTS steel): (a) Mean corrosion depth=2 mm; (b) Mean corrosion depth=4 mm.

CONCLUSIONS

A series of nonlinear elastic-plastic finite element analyses has been performed on the plates in different conditions of un-corroded, uniformly corroded and randomly corroded. The plates have been subjected to in-plane compression load. Full-range average stress-average strain relationships of the plates have been derived considering the changes in plate aspect ratio, plate slenderness or thickness,

mean corrosion depth and standard deviation of random thickness variation. The results can be summarized as follows:

- The buckling and ultimate strengths for any group of 50 models analysed in each of the above-mentioned cases are almost insensitive to the random thickness variations over the plate surfaces.
- By changing the type of material from HTS steel to NS steel, the amounts of reductions in the buckling strengths are generally diminished.
- For any group of the 50 analysed plate models in each of above-mentioned cases, the post-ultimate-strength regions of the average stress-average strain relationships create a band. The band width is generally decreased with changing the plate aspect ratio from 3 to 2.
- In each case, the trends of the curves in the post-ultimate-strength region are similar.
- Aspect ratio, thickness and also random corrosion parameters have different effects on the strength characteristics of the corroded plate. Random corrosion has the weakening effects on the buckling and ultimate strengths of the plate. The case of uniform corrosion leads to an intermediate condition for the plate with different probable random thickness variations.
- In order to investigate the strength characteristics of the randomly corroded plate under the longitudinal in-plane compression, without any modelling of the random thickness variations, a practical proposal was developed to calculate the effective thickness of the plate.

REFERENCES

1. Nakai, T., Matsushita, H., Yamamoto, N., et al. (2004), "Effect of pitting corrosion on local strength of hold frames of bulk carriers (1st report)", *Mar. Struct.*, no. 17, p. 403–432.
2. ASM International Corrosion. (2001), "ASM Handbook", vol. 13.
3. Mateus, A.F., Witz, J.A. (1997), "On the post-buckling of corroded steel plates used in marine structures", *Trans. RINA*, 140, 165–83.
4. Daidora, J.C., Parente, J., Orisamolú, I.R., Ma K.T. (1997), "Residual strength assessment of pitted plate panels", *Ship Structure Committee*, SSC-394.
5. Slater, P.A., Pandey, M.D., Sherbourne, A.N., "Finite element analysis of buckling of corroded ship plates", *Can. J. Civ. Eng. CSCE*, 2000, 27, 463–474.
6. Paik, J.K., Lee, J.M., Ko, M.J. (2003), "Ultimate compressive strength of plate elements with pit corrosion wastage", *J. Eng. Mar. Environ.*, 217(M4), 185–200.
7. Paik, J.K., Lee, J.M., Ko, M.J., "Ultimate shear strength of plate elements with pit corrosion wastage", *Thin-Wall. Struct.*, 2004, no. 42, p. 1161–1176.
8. Ok, D., Pu, Y. and Incecik, A. (2007), "Computation of ultimate strength of locally corroded unstiffened plates under uniaxial compression", *Mar. Struct.*, 20, 100–114
9. Cyr, R.R.J., Akhras, G., "Buckling of corroded stiffened steel plates", *Proceedings of CSME*, 2004, p.802–9.
10. Akhras, G., Cyr, R., "Testing corroded stiffened steel plates for ultimate strength", *Proceedings of the fifth structural specialty conference CSCE*, 2004, ST-188.
11. Nakai, T., Matsushita, H., Yamamoto, N. (2004), "Effect of pitting corrosion on local strength of hold frames of bulk carriers (2nd report). Lateral–distortional buckling and local face buckling", *Mar. Struct.*, 17, 612–641.
12. Dunbar, T.E., et al., "A computational investigation of the effects of localized corrosion on plates and stiffened panels", *Mar. Struct.*, 2004, p. 17(5), no. 385–402.
13. Amlashi, H.K.K., Moan, T., "On the strength assessment of pitted stiffened plates under biaxial compression loading", *24th international conference on offshore mechanics and arctic engineering*, Halkidiki, Greece, 2005.
14. ANSYS Inc., "ANSYS 11.0 Reference Manual", 2008.
15. Khedmati, M.R., "Ultimate strength of ship structural members and systems considering local pressure loads", *Dr. Eng. Thesis, Graduate School of Engineering, Hiroshima University*, 2000.

Fujikubo, M., Yao, T., Khedmati, M.R., Harada, S., Yanagihara, D., “Estimation of ultimate strength of continuous stiffened panel under combined transverse thrust and lateral pressure, Part 1: Continuous plate”, *Marine Structures*, 2005, no. 18, p. 383–410.

16. Fujikubo, M., Harada, S., Yao, T., Khedmati, M.R., Yanagihara, D., “Estimation of ultimate strength of continuous stiffened panel under combined transverse thrust and lateral pressure, Part 2: Continuous stiffened panel”, *Marine Structures*, 2005, no. 18, p. 411–417.

17. Ueda, Y. and Yao, T., “The influence of complex initial deflection on the behaviour and ultimate strength of rectangular plates in compression”, *J. of Const. Steel Research*, 1985, no. 5, p. 265-302.

18. Yao, T., Nikolov, P.I. and Miyagawa, Y., “Influence of welding imperfections on stiffness of rectangular plates under thrust”, *Proc. of IUTAM Sump. on Mechanical Effects of Welding*, (Eds.: Karlsson, K., Lindgren, L.E. and Jonsson, M.), Springer-Verlag, 1992, p. 261-268.

19. Khedmati, M.R. and Karimi, A.R., “Ultimate compressive strength of plate elements with randomly distributed corrosion wastage”, *Proceeding of the Eight International Conference on Computational Structural Technology*, 2006, (Eds.: Topping, B.H.V., Montero, G. and Montenegro R.), Civil-Comp Press.

20. Distributed corrosion wastage”, *Proceeding of the Eight International Conference on Computational Structural Technology*, (Eds.: Topping, B.H.V., Montero, G. and Montenegro R.), Civil-Comp Press.

21. Ghavami, K., “Experimental study of stiffened plates in compression up to collapse”, *J. of Const. Steel Research*, 1994, no. 28(2), p. 197-222 [Special Brazilian Issue, Guest Editor Khosrow Ghavami].

22. Ghavami, K. and Khedmati, M.R., “Numerical and experimental investigations on the compression behaviour of stiffened plates”, *J. of Const. Steel Research*, 2006, no. 62(11), p. 1087-1100.

23. Fujikubo, M., Yao, T., Khedmati, M.R., “Estimation of ultimate strength of ship bottom plating under combined longitudinal thrust and lateral pressure”, *Trans. West Japan Soc. Nav. Architects*, 1999.

24. Antonio F. Mateus., Joel A. Witz., “On the Influence of Thickness Variation on the Post-Buckling Behaviour of Corroded Steel Plates”, *The Royal Institution Of Naval Architects*, London, 2001.